NASA Technical Memorandum 101576

NOISE RADIATION CHARACTERISTICS OF THE WESTINGHOUSE WWG-0600 (600kW) WIND TURBINE GENERATOR

KEVIN P. SHEPHERD
HARVEY H. HUBBARD

JULY 1989

National Aeronautics and
Space Administration

Langley Research Center
Hampton, Virginia 23665-5225

INTRODUCTION

There is a need to develop a data base for evaluating the environmental impact of mid-range (100-1000 kW output) horizontal axis wind turbine generators of the types proposed for future wind power stations. The Westinghouse WWG-0600 machine is believed to be representative of those mid-range machines for which limited acoustic data are available (see Refs. 1-6). References 1, 2, 3 and 4 contain narrowband and broadband spectra and directivity patterns for the 200kW MOD-0A Department of Energy machine and its research version, the MOD-0 machine, which was operated at two rotational speeds as well as in the upwind and downwind configurations. Reference 5 presents fragmentary spectral data at various distances (upwind and downwind) and for several wind speeds for the Danish NIBE 640 kW machine and the Danish Windane 300 kW machine. Reference 6 contains detailed spectral information for the Danish Danwin machine as well as for several smaller machines of American and foreign manufacture. The noise characteristics of the 600 kW WWG-0600 machine are believed to be of direct interest to those involved in wind power station siting and development in proximity to communities (Ref. 7).

The present study makes use of a currently operating wind power station to obtain systemmatic acoustic measurements for a range of power output/wind speed conditions. The data are compared with results for other similar machines and with predictions by available methods.

This effort is part of the Department of Energy wind energy program managed by the Solar Energy Research Institute. Data were obtained with the assistance and cooperation of Hawaiian Electric Co. personnel at the site.

APPARATUS AND METHODS

Description of Machine

The WWG-0600 machine is an upwind horizontal axis configuration with a two-bladed 43.3 m diameter teetering rotor mounted on a 2 m diameter circular cross section tower. The rotor has 0^{o} coning, a tilt angle of 4^{o} and a total blade twist of 6.75^{o}. Hub height is 36.6 m. Blades are laminated wood with a linear taper from 0.8 m at the tip to 1.1 m at the root. The machine operates at a constant 43 rpm with a fundamental blade passage frequency of 1.43 Hz. Its rated output power at 10.3 m/s wind speed is 600 kW and its operational range of wind speeds is between 5.2 m/s (cut-in) and 18.4 m/s (cut-out).

During the tests, wind speed, wind direction and output power were recorded for correlation with the acoustic data. Figure 1 is a photograph of one of the machines in operation, showing the nature of the vegetation and ground surface in its vicinity.

Description of the Site

The test site is located in the Kahuku region of Oahu, HI (see figure 2). Fifteen WWG-0600 machines are located along ridge lines at elevations ranging from 150 to 250 m above sea level. Those machines for which data are included in this paper are identified by the circle symbols. Those shown as the squares either were not operating or the adjacent terrain was not acceptable for making measurements.

The ridge lines are generally parallel to each other, are generally perpendicular to the prevailing wind and are located about 5.5 km from the sea coast in the downwind direction. The ground surface surrounding each of the five machines for which data were obtained is flat in the crosswind direction and generally slopes sharply downward away from each machine in the upwind and downwind directions. Data were obtained from five different machines in the array.

Trade winds were from the east to northeast and blew steadily in the range 15-30 mph (6.7-13.4 m/s) during the tests. Wind speed values are 30 second averages from nacelle mounted anemometer readings adjusted for rotor blade blockage effects.

Figure 3 illustrates the contours of the land in the vicinity of one of the test machines. Shown are the elevations as a function of distance from the machine in the upwind direction. It can be seen that the terrain is very uneven with the result that the incoming wind passes over a succession of ridges and valleys before encountering the rotor disk. Although the details may be different for other machines, the data of the figure are generally representative.

Noise Measurements and Analyses

Noise measurements were made with commercially available battery powered instrumentation. One-half inch diameter condenser microphones with a useable frequency range of 3-20,000 Hz were used with a four channel FM tape recorder having a useful dynamic range of 40 dB in the frequency range of 0-15000 Hz. For cases where low frequency (f=2.8-4.2 Hz) rotational harmonic levels are plotted in the figures the levels are adjusted for microphone response.

Acoustic data were obtained for distances from about 60 to 80 m and at various azimuth angles around the machines for daytime operations over a range of power outputs. All acoustic data were recorded on magnetic tape for later analyses. Spectral data were obtained with the aid of conventional one-third octave and narrow band analyzers.

To minimize the detrimental effects of wind noise, polyurethane foam microphone wind screens were used and microphones were placed at the ground surface, where wind velocities were relatively low. Background noise levels were sufficiently low that adequate signal to noise ratio existed for all broadband noise data included herein.

RESULTS AND DISCUSSION

Data are presented in the form of one-third octave band spectra, narrow band frequency spectra, and directivity plots using one-third octave band levels and A-weighted levels. Measured results for the WWG-0600 machine are compared with calculations by available methods and also with similar measured data from other wind turbines.

Broadband Noise Components

Example Spectra - The effects of output power/wind speed are illustrated by the one-third octave band spectra of figure 4 (a), (b) and (c). Included are data at three different azimuth angles, ß, from the machine (see inset of figure 1) for a range of power outputs. The spectra are similar in shape for all test conditions upwind and downwind. The spectra peak in the frequency range near 10 Hz and the levels generally decrease in value as frequency increases. Broad band components are noted to dominate the spectra except for the 30 Hz band which contains the fundamental generator shaft harmonic (observed only in the crosswind direction) and for the very low frequency bands which contain some rotational harmonics. A general result is that the highest sound pressure levels are associated with the highest power outputs/wind speeds.

Comparisons with Calculations - Calculations of broad band noise have been made by the method of Ref. 8 and the results are shown in figures 5 (a) and (b), for locations at $ß=0^{o}$ and 180^{o}; and for both high and low power conditions. The data points of figure 5 (a) represent measured one-third octave band spectra for 4 different test runs on 3 individual machines. The solid curve represents the calculated values for this high power output condition. It can be seen that the spectral shape and levels are in good agreement with measurements. Comparable results for 3 individual machines are shown in figure 5 (b) for the low power case and calculations are seen to generally underpredict the measurements at the lower frequencies.

Radiation Patterns - The data of figures 6 and 7 characterize the noise radiation properties of the WWG-0600 machine. Figure 6 shows the polar distribution of sound pressure levels for various one-third octave bands. For the band levels shown, the upwind and downwind values are nearly equal and both are generally 3-5 dB higher than the crosswind values.

A similar result is shown in figure 7 for the "A"-weighted sound pressure levels. Data are presented for a high power range and a low power range for comparison. Upwind and downwind levels are essentially equal and are slightly higher than crosswind levels.

Comparisons with Other Machines - Data are presented in figure 8 at the same reference distance so that comparisons can be provided for three different horizontal axis machines of similar size and power output. The shaded region indicates the range of sound pressure levels for two power output values for the WWG-0600 machine namely, 96 kW (bottom boundary) and 600 kW (top boundary). Shown for comparison are individual spectra for the MOD-OA (Ref. 3) and the DANWIN (Ref. 6) machines, along with their associated rated output powers and tip speeds, normalized to a reference distance of 2.5 diameters. All of the spectra are seen to have generally the same shapes except that of the DANWIN machine which has a large machinery noise component near 500 Hz. The levels would be expected to be comparable for similar operating conditions. Differences in tip speed generally account for the differences seen in the figure.

Discrete Frequency Noise Components

Narrow Band Spectra - The effects of output power/wind speed are further illustrated by the narrow band width (Δf = 0.125 Hz) spectra of figure 9 which show those components below 100 Hz. Figure 9 (a) identifies some of the discrete frequency peaks. Generator shaft fundamental (30 Hz) and its harmonics are easily seen at the lower power condition where the broad band noise levels are relatively low. These shaft harmonics are identifiable mainly in the direction of the rotor plane ($\beta = 90^{o}$), and are seen less clearly at $\beta=0^{o}$

(upwind) in figure 9(b) and at ß=180° (downwind) in figure 9(c). Also seen are a number of rotational harmonics which occur at the blade passage frequency (1.43 Hz) and integer multiples of it. Although the rotational harmonics are more easily identified at the lower power conditions they are present for all power conditions and at all of the measurement locations for which data were obtained. Thumping noises observed during the tests probably resulted from the rotational harmonics.

Comparisons of Measured and Calculated Rotational Noise Levels - The presence of relatively strong rotational noise harmonics for all test conditions and measurement locations was an unexpected result for an upwind configuration of a horizontal axis machine. One possible cause of the enhancement of these low frequency rotational harmonics is a non-uniform inflow to the rotor, although no direct wind speed gradient measurements were available for this site. Reference 9, based on previous developments by Sears (Ref. 10) and Lowson (Ref. 11), contains a procedure for calculation of the rotational noise harmonics of a wind turbine which includes the effects of wind speed gradients. Several assumed wind profiles, shown in figure 10, were used as inputs to the calculations in an attempt to evaluate wind speed gradient effects. Profiles A, B and C, are referred to as disk shadow profiles since the wind speed is assumed constant over the rotor disk except for a small shadowed portion at the bottom, within which all wind speed gradients occur. Profiles D and E are included as less drastic wind gradient profiles. Profile D corresponds to the 1/7th power relation for turbulent flow over a smooth surface (Ref. 12). Profile E is estimated, based on the results of Ref. 13, to represent turbulent flow over a rough ground surface. Results of calculations based on the above wind speed profiles and the assumption that the aerodynamic forces on the rotor blades are concentrated at the 0.75 radius station, are shown in figures 11, 12, 13 and 14.

Example calculated rotational noise spectra are shown in figure 11. The spectral curves, in each case, connect the calculated levels of the harmonics. Curves for profiles D

and E are seen to slope sharply downward, thus indicating essentially no harmonic content. The curve for profile B corresponds to an assumed disk shadow angle, α, of 45^{o} and a wind speed deficit, V_d, in the shadowed area on the disk, of 3.6 m/s. The calculated levels for the more drastic wind profile B are much higher than those for profiles D and E. The harmonic levels are seen to cycle from low to high to low every fourth harmonic, the interval being related to the assumed shadow angle. For a more restricted shadow the above intervals are longer. A spectrum envelope line is drawn through the individual peak calculated values.

Computed spectrum envelopes for profiles A, B and C, a wind speed deficit (V_d) of 3.6 m/s and a disk shadow angle of 45^{o} are shown in figure 12 along with measured data. The measurements show about ± 5 dB of scatter for a range of wind speeds/power outputs. They reduce in level generally at the higher harmonic orders and tend to cluster around the spectrum envelope corresponding to profile B. By inference, the relatively high rotational harmonic measured levels seem to result from shadowing of the rotor disk such as might be caused by terrain induced distortion. The spectral oscillation interval from the data appears to correspond to a shadow angle of 45^{o} but this is only found at low power conditions and is not a well defined result.

Further calculations were made for other values of assumed disk shadow angle and velocity deficit in the disk shadow. The resulting spectrum envelopes, plotted in figure 13, illustrate that higher sound pressure levels result from greater velocity deficits and from more restricted disk shadow angles.

Some example calculated radiation diagrams are shown in figure 14 along with comparable experimental data. Figures 14 (a), (b) and (c) present results for rotational harmonic (m) values of 2, 4 and 8 respectively. Note that the calculations give axially symmetric patterns having equal values upwind and downwind on the axis. Slightly higher

values are associated with the downwind quadrants and relatively low values are predicted near the plane of rotation. The experimental data show considerable scatter but suggest that the rotational harmonic noise radiates about equally in all directions. Agreement with the calculations is good for rotational harmonic values of 2 and 4 on the axis and is poor in the plane of rotation. The calculated values for m=8 are lower than the measured values in all directions.

CONCLUDING REMARKS

The WWG-0600 noise spectra peak at the lower frequencies and the levels generally reduce as frequency increases, as do those of other similar machines for which data are available. Both broadband and narrowband components were identified in the WWG-0600 noise spectra for all test conditions and also for all measurement locations. The higher noise levels of both broadband and discrete frequency components are generally associated with the higher power outputs/wind speeds.

The broadband components tend to have their highest levels at the lower frequencies and to gradually decrease in level as the frequency increases. Predictions of broadband noise are in good agreement with the measurements at high output power values but underestimate the measurements at low output power values.

Discrete frequency components at integer multiples of the blade passage frequency (rotational noise harmonics) which have not been measured for other similar machines, are identified in all of the measured spectra. Calculations indicate that the above phenomenon results from a shadowing of the rotor disk as a result of terrain induced inflow distortion. Predictions of narrowband noise levels are in general agreement with the measurements at directly upwind and downwind locations but underestimate the measurements in the plane of the rotor.

REFERENCES

1. Etter, C. L., Kelley, N. D., McKenna, H. E., Linn, C. and Garrelts, R.: Acoustical Measurements of DOE/NASA MOD-0 Wind Turbine at Plum Brook Station, Ohio. Solar Energy Research Inst., SERI/TR-635-1240, June 1983.

2. Hubbard, Harvey, H., Grosveld, F. W. and Shepherd, Kevin P.: Noise Characteristics of Large Wind Turbine Generators. Noise Control Engineering Journal, Vol. 21, No. 1, pp. 21-29, 1983.

3. Shepherd, K. P. and Hubbard, H. H.: Sound Measurements and Observations of the MOD--0A Wind Turbine Generator. NASA CR-165856, February 1982.

4. Balombin, J. R.: An Exploratory Survey of Noise Levels Associated with a 100kW Wind Turbine NASA TM 81486, 1980.

5. Kristensen, J.: Noise Measurements Around the NIBE (Denmark) Wind Turbines and the WINDANE 31 wind Turbine. Aero. Res. Inst. of Sweden Proc. of the IEA Workshop on Wind Turbine Noise Measurements, Stockholm, November 1984.

6. Anonymous: Measurement and Evaluation of Environmental Noise from Wind Energy Conversion Systems in Alameda and Riverside Counties. Wyle Laboratories Research Report, WR 88-19, October 1988.

7. Shepherd, K. P. and Hubbard, H. H.: Prediction of Far Field Noise from Wind Energy Farms. NASA CR 177956, April 1986.

8. Grosveld, F. W.: Prediction of Broadband Noise from Large Horizontal Axis Wind Turbines. AIAA Journal of Propulsion and Power. Vol. 1, No. 4, July-August 1985.

9. Viterna, Larry A.: The NASA-LERC Wind Turbine Noise Prediction Code. NASA CP-2185, February 1981.

10. Sears, William R.: Some Aspects of Non-Stationary Airfoil Theory and Its Practical Applications. J. Aeron. Sci. 85, 1941.

11. Lowson, M. V.: Theoretical Analysis of Compressor Noise. J. Acous. Soc. of Amer., 47, 1 (Part 2) pp. 371-3875, 1970.

12. Sutton, O. G.: Micrometeorology. McGraw Hill Book Co.,London, England, 1953.

13. Frost, W. and Shieh, C.: Guidelines for Siting WECS Relative to Small-Scale Terrain Features. Final Report, FWG Asso. Inc., Tullahoma, TN, February 1981.

Figure 1. - Photograph of a Westinghouse WWG-0600 wind turbine installation at the Kahuku, HI test site with insert diagram showing locations of measurement points.

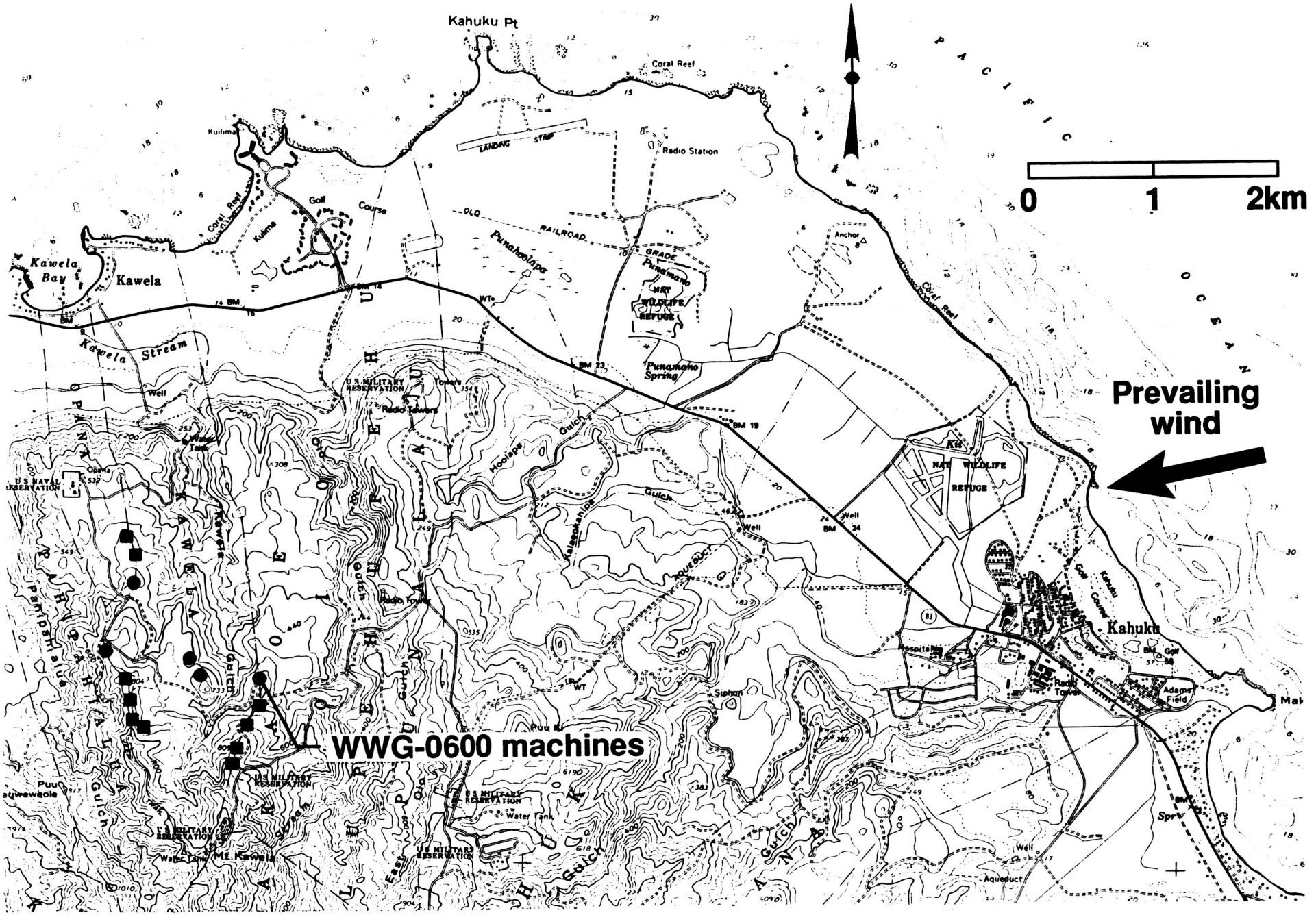

Figure 2. - Locations of WWG-0600 machines in the Kahuku, HI test area.

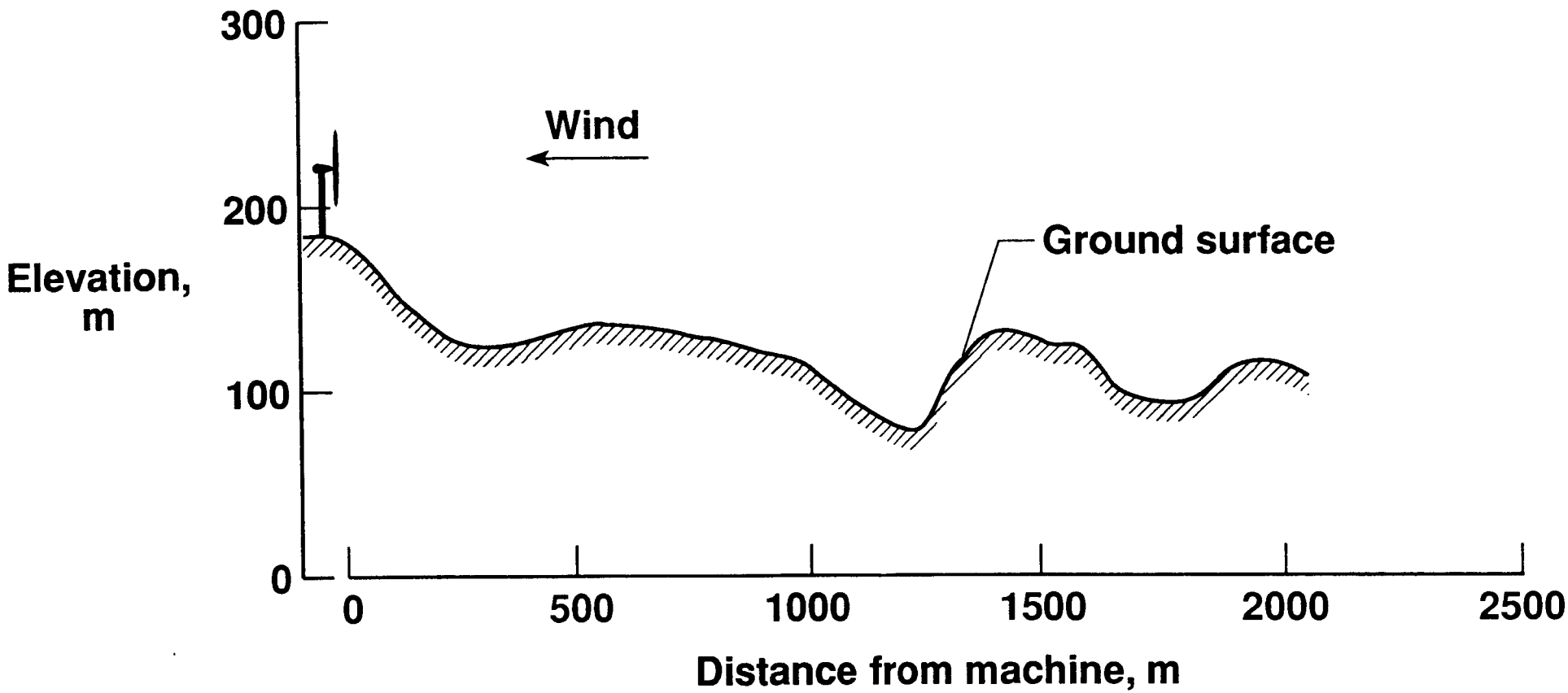

Figure 3. - Ground surface profile upwind of WWG-0600 machine.

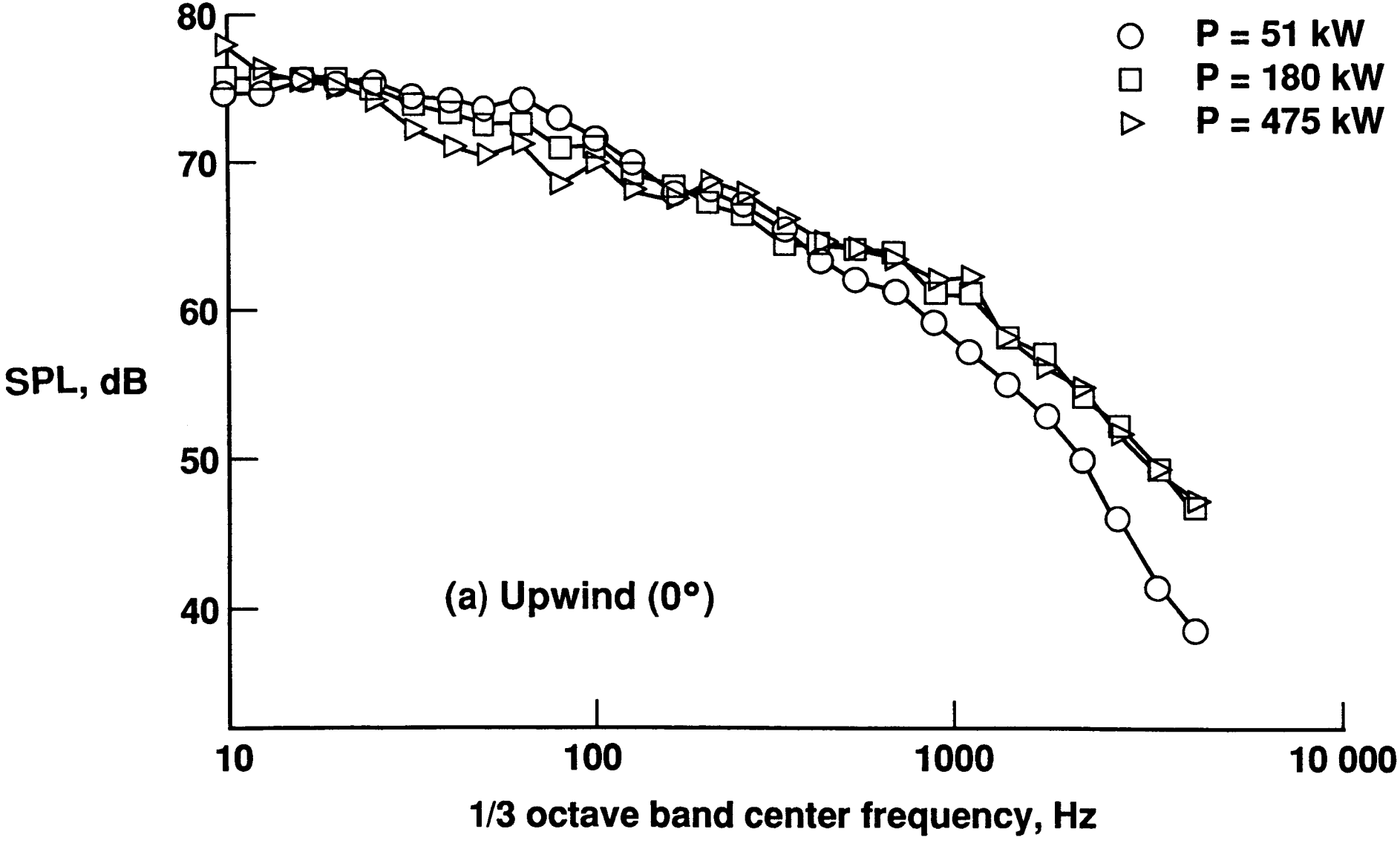

Figure 4. - One-third octave band spectra for the WWG-0600 machine for a range of power outputs at three azimuth angles. d = 65 m.

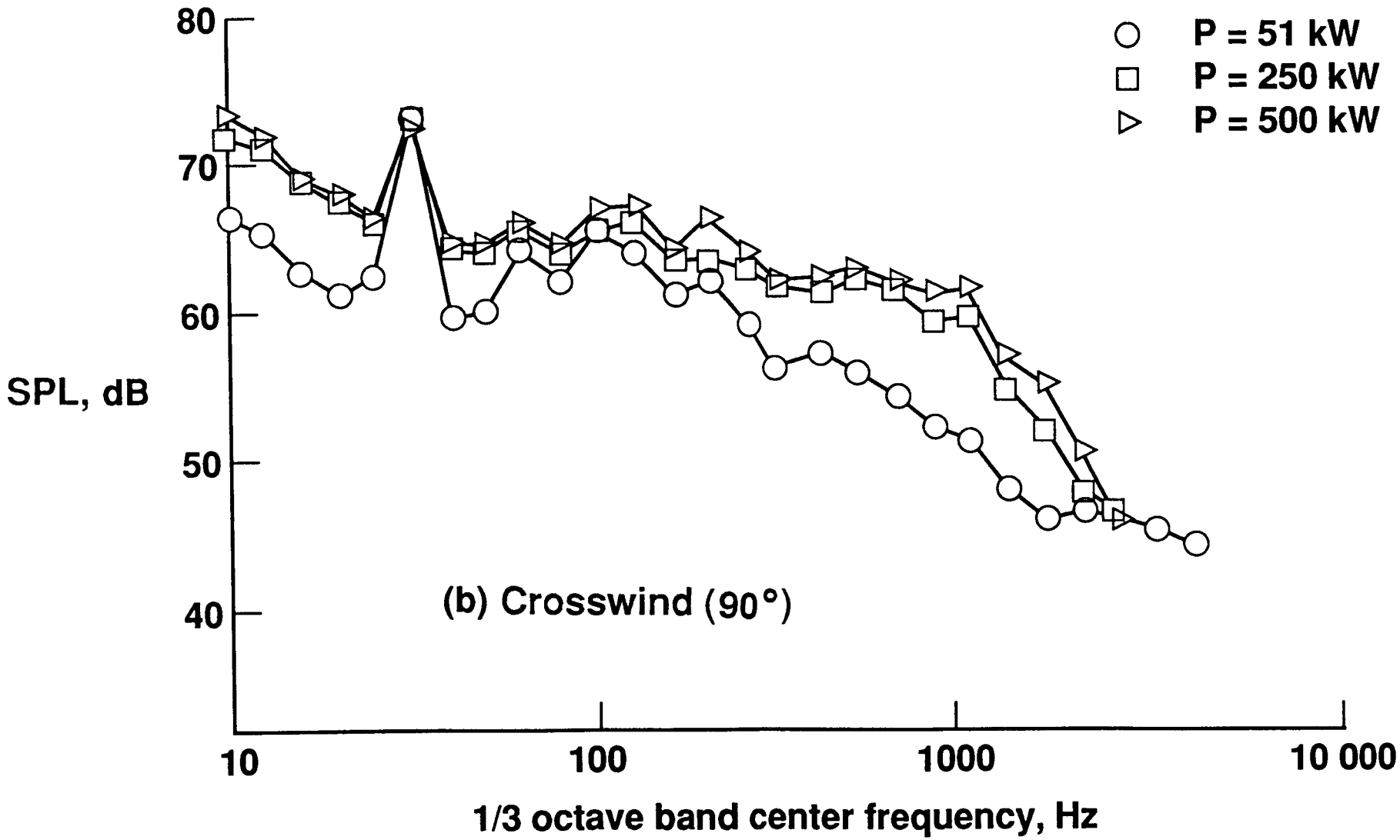

Figure 4. - (Cont.)

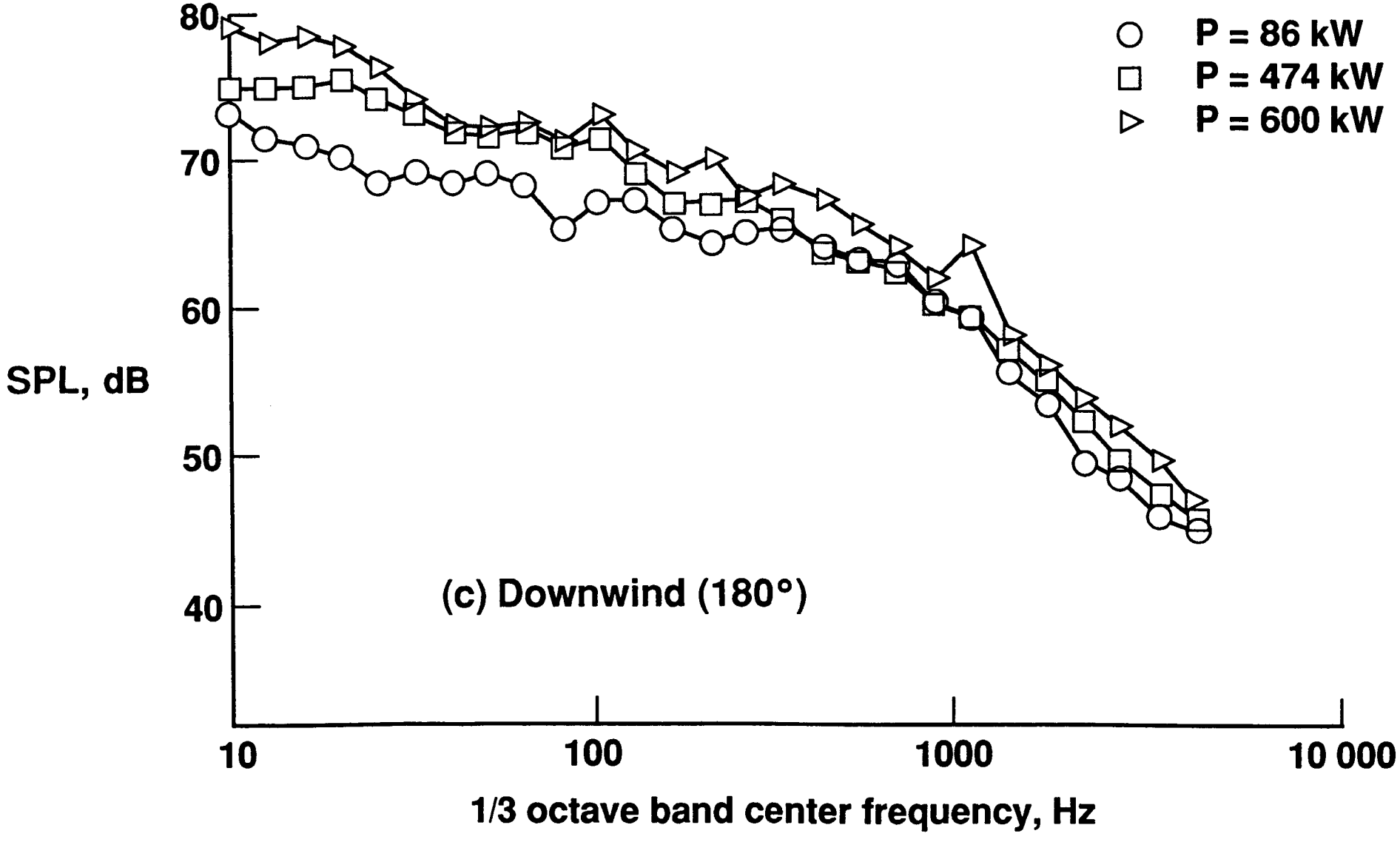

Figure 4. - (Concl.)

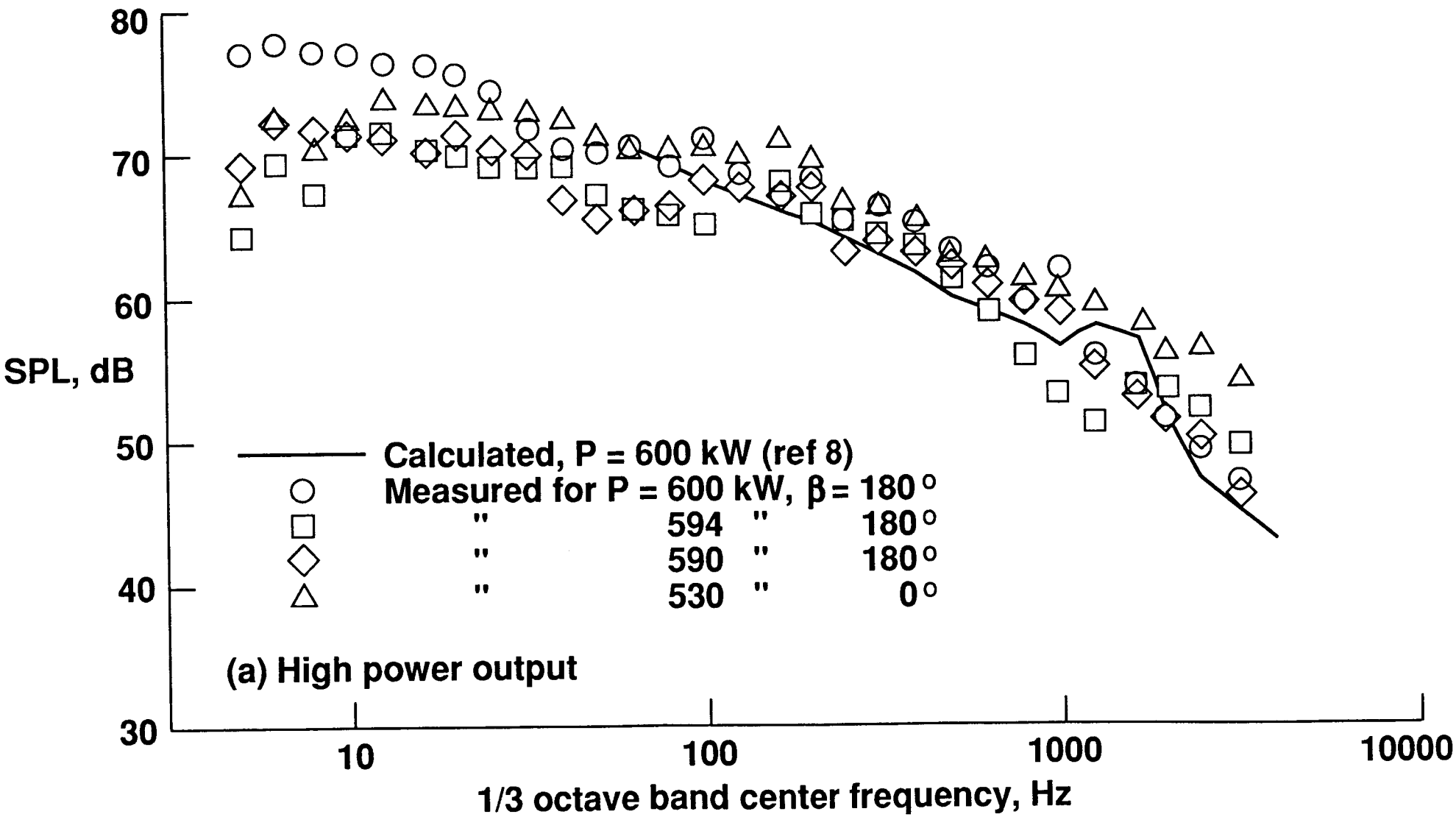

Figure 5. - Comparisons of on-axis measured and calculated one-third octave band spectra for WWG-0600 machine at both high and low output power conditions. d = 65 m.

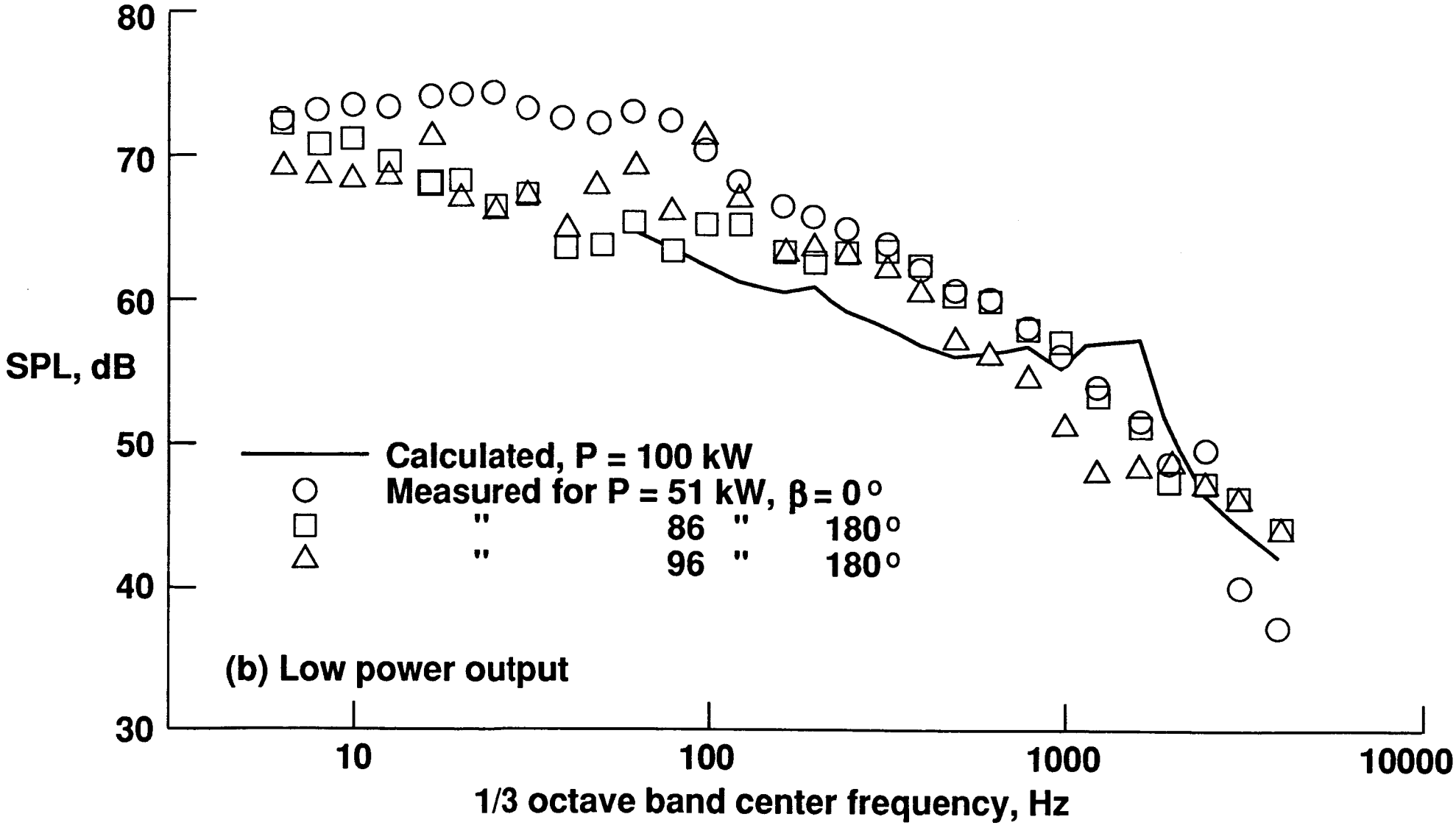

Figure 5. - (Concl.)

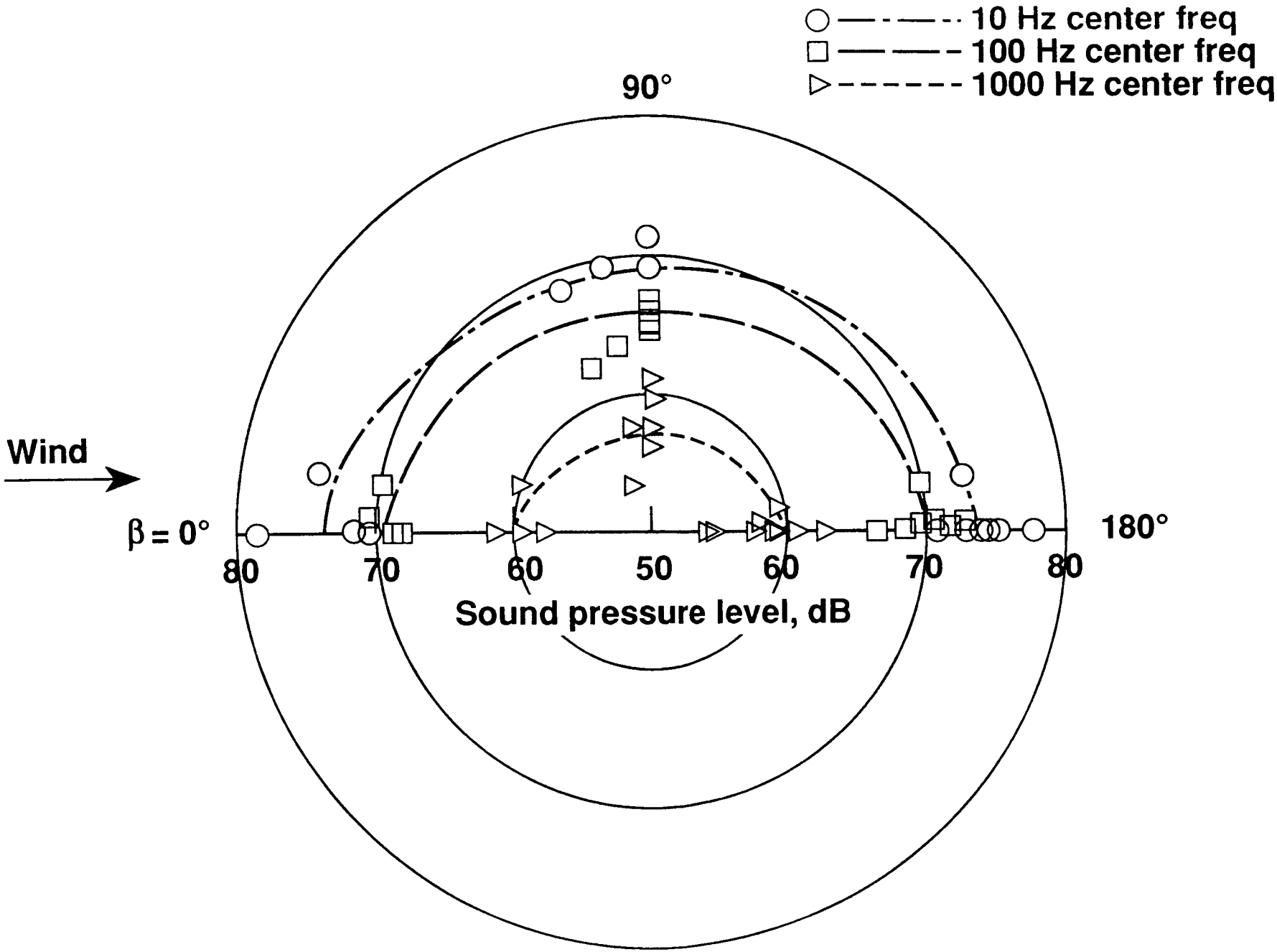

Figure 6. - Polar distribution of sound pressure levels in three different one-third octave bands for the WWG-0600 machine. V = 8.1 - 13.4 m/s, P = 280-600 kW, and d = 65 m.

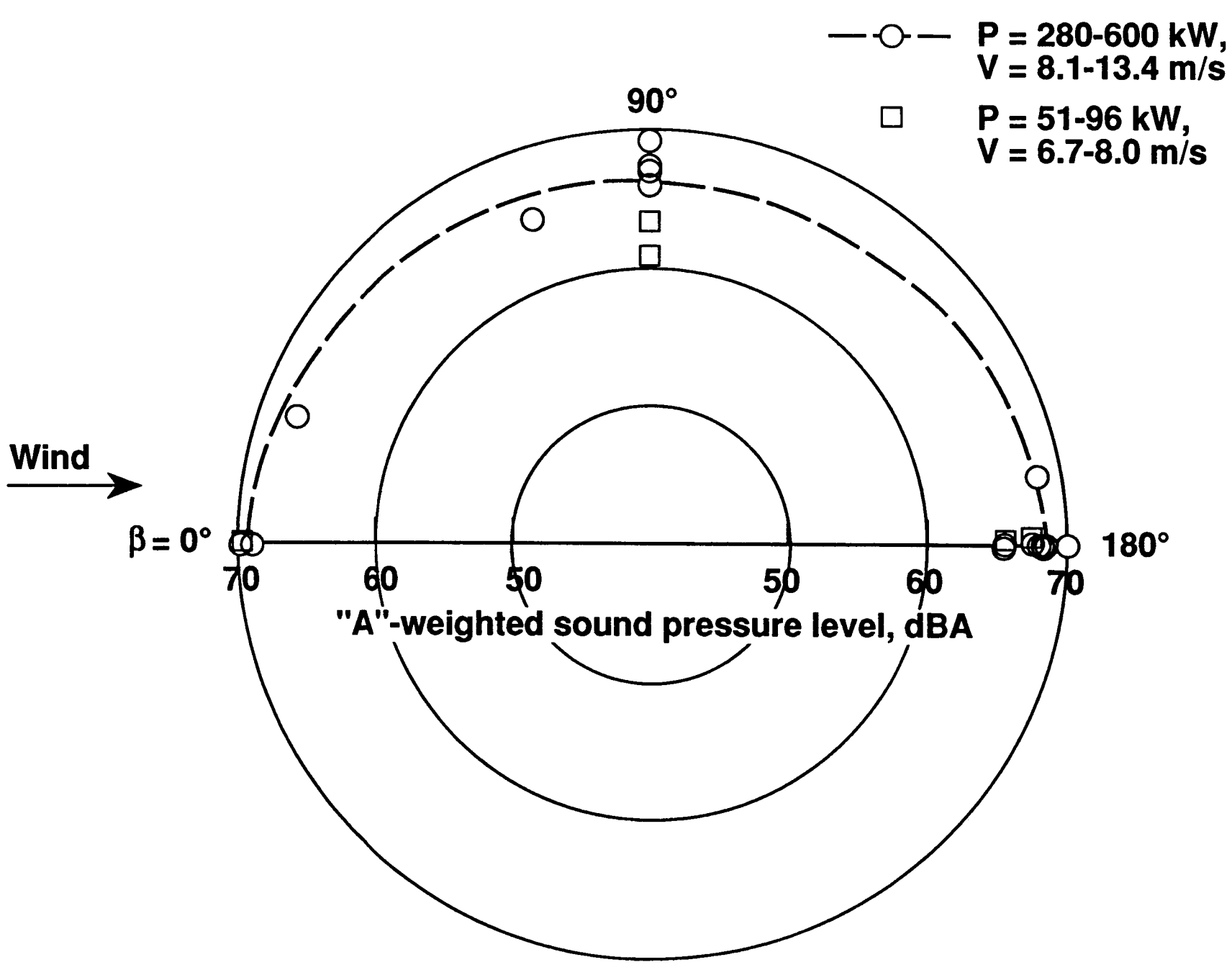

Figure 7. - Polar distributions of "A"-weighted sound pressure levels for the WWG-0600 machine. d = 65 m.

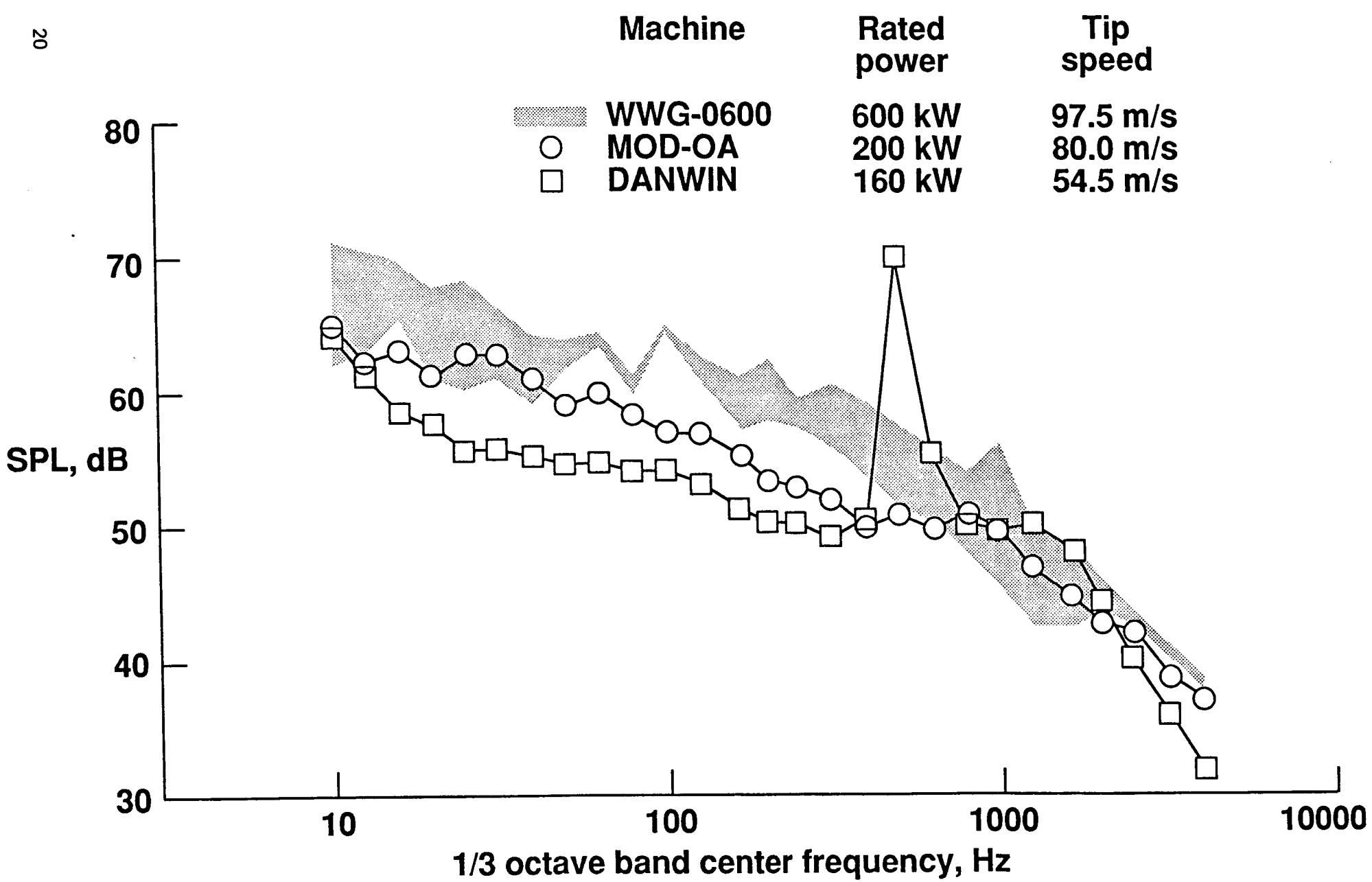

Figure 8. - Comparisons of measured on-axis one-third octave band spectra for three mid-range machines at a slant range reference distance of 2.5 diameters.

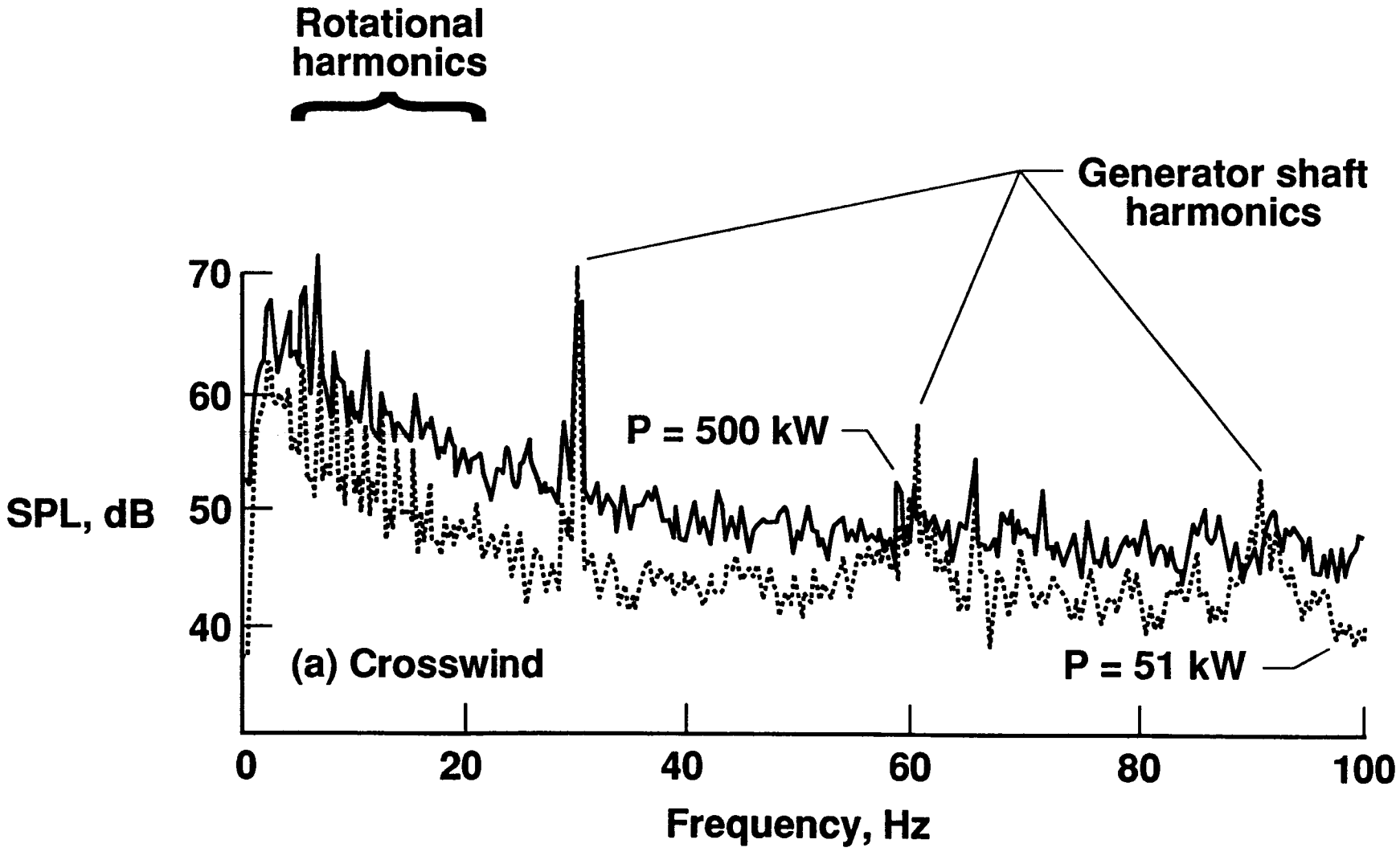

Figure 9. - Example narrow band Δf = 0.125 Hz) spectra for the WWG-0600 machine at both high and low power outputs for three azimuth angles. d = 65 m.

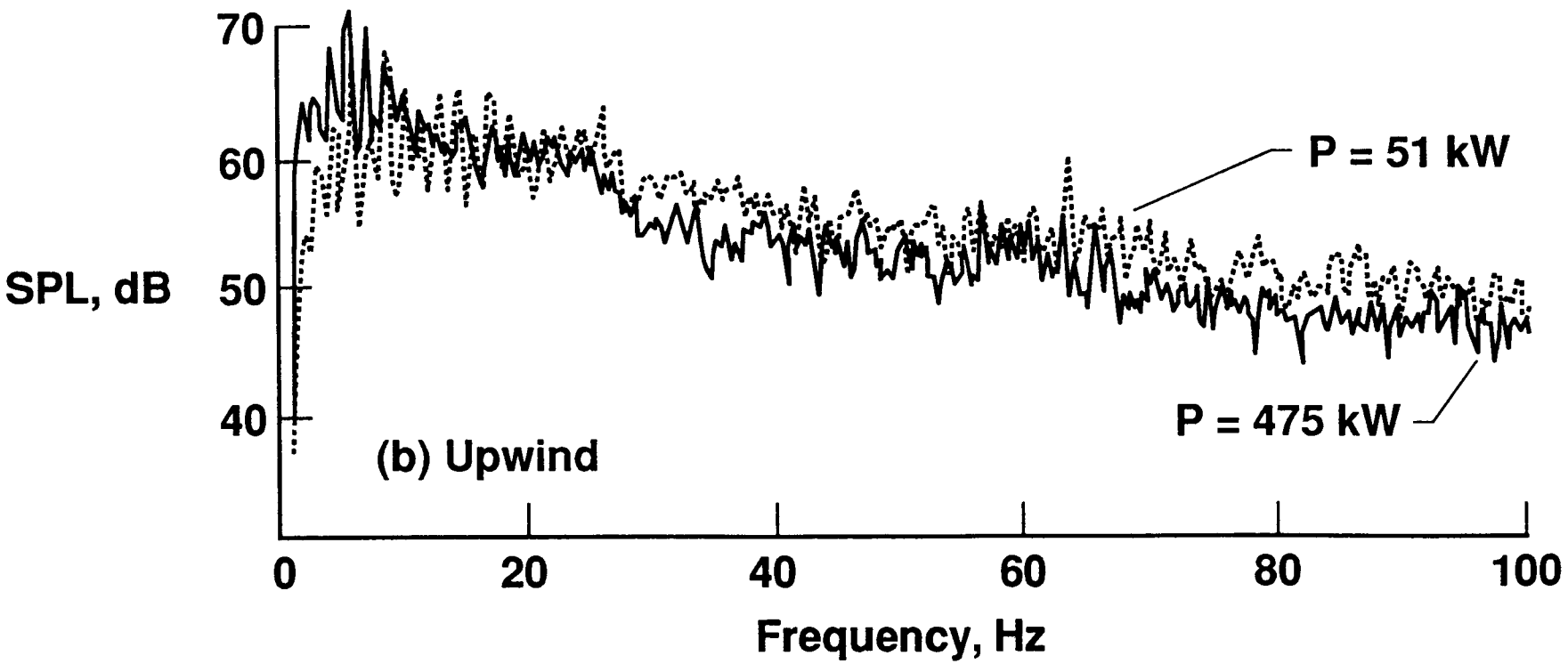

Figure 9. - (Cont.)

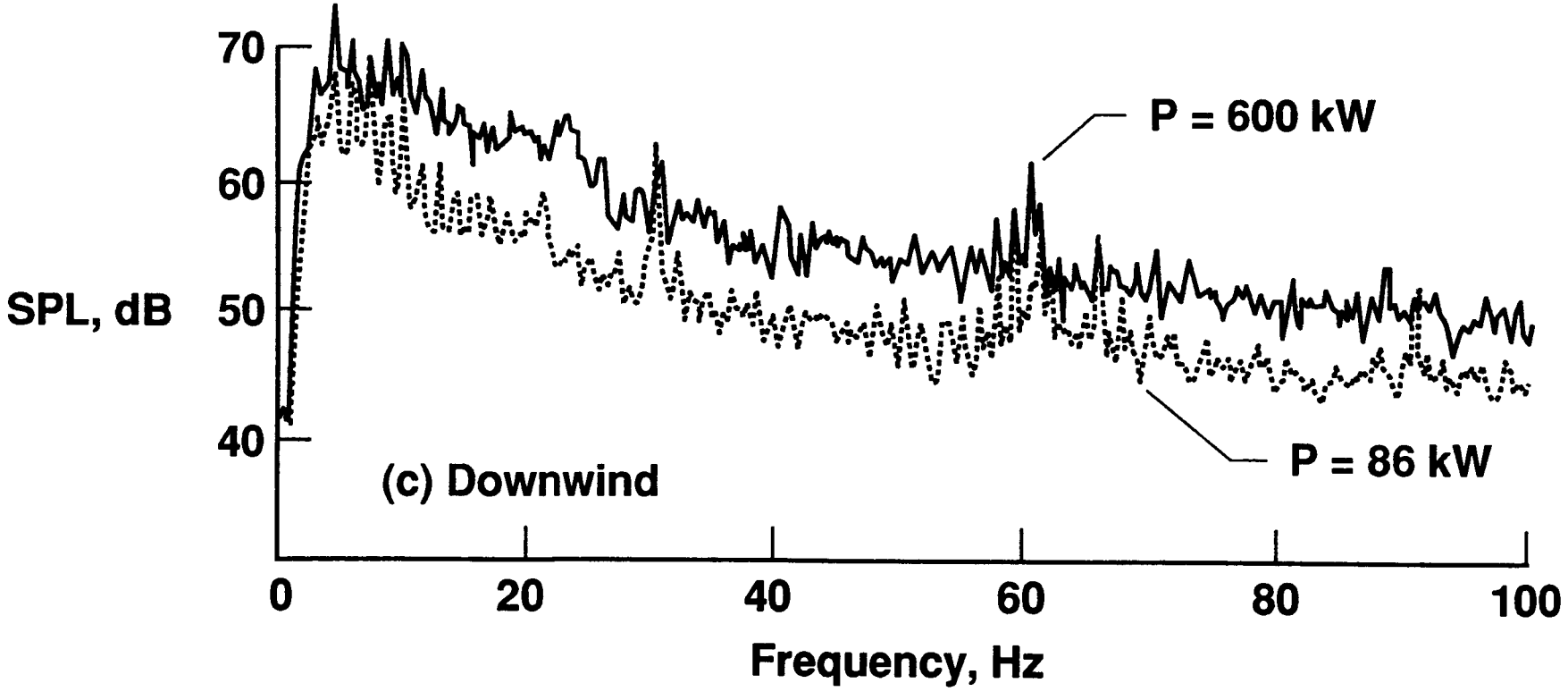

Figure 9. - (Concl.)

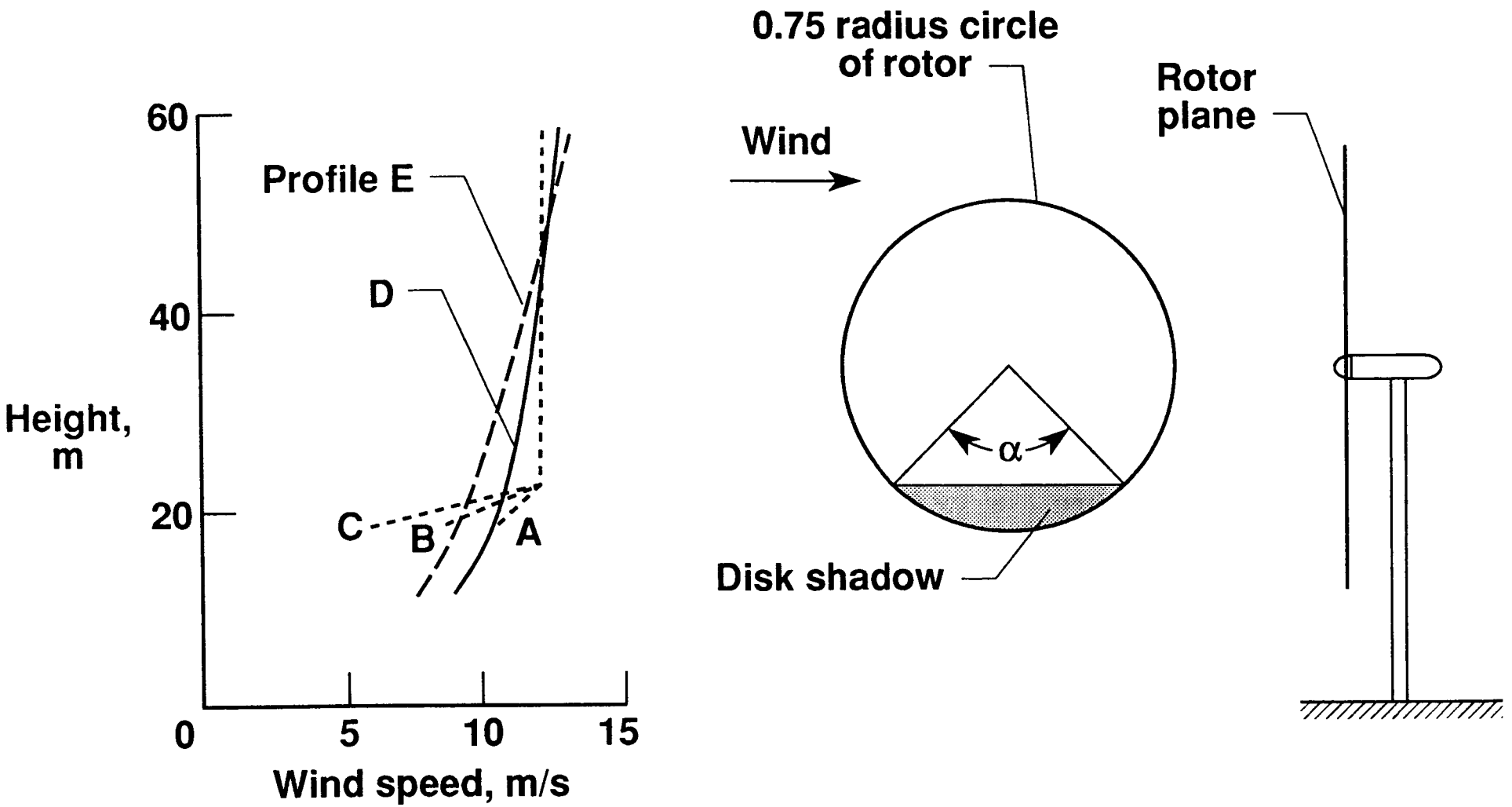

Figure 10. - Assumed wind gradient inputs to WWG-0600 rotational noise harmonic calculations.

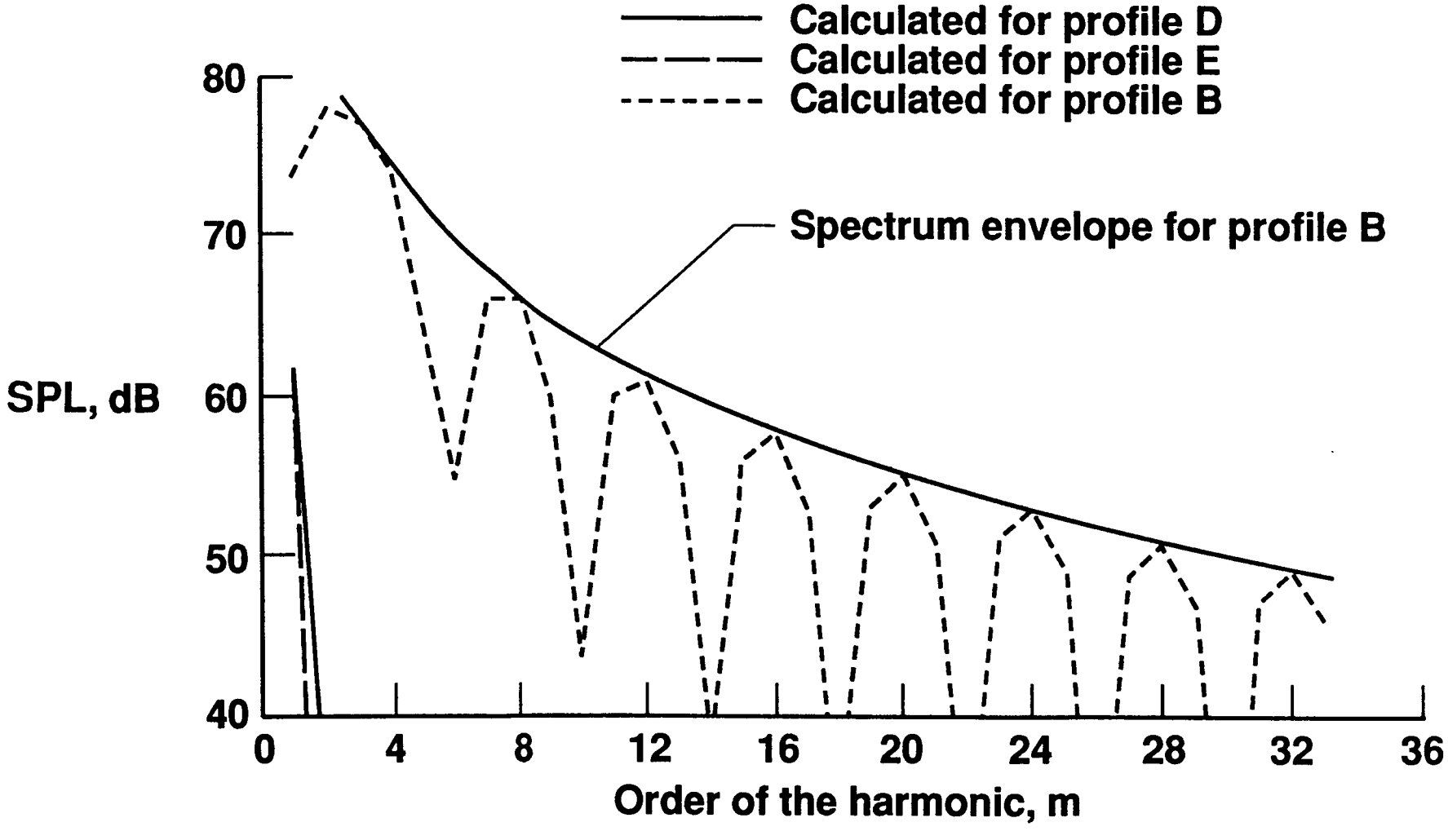

Figure 11. - Calculated rotational noise spectra for WWG-0600 machine for assumed disk shadow profiles of figure 10, using the method of Ref. 9. P = 600 kW, d = 65 m.

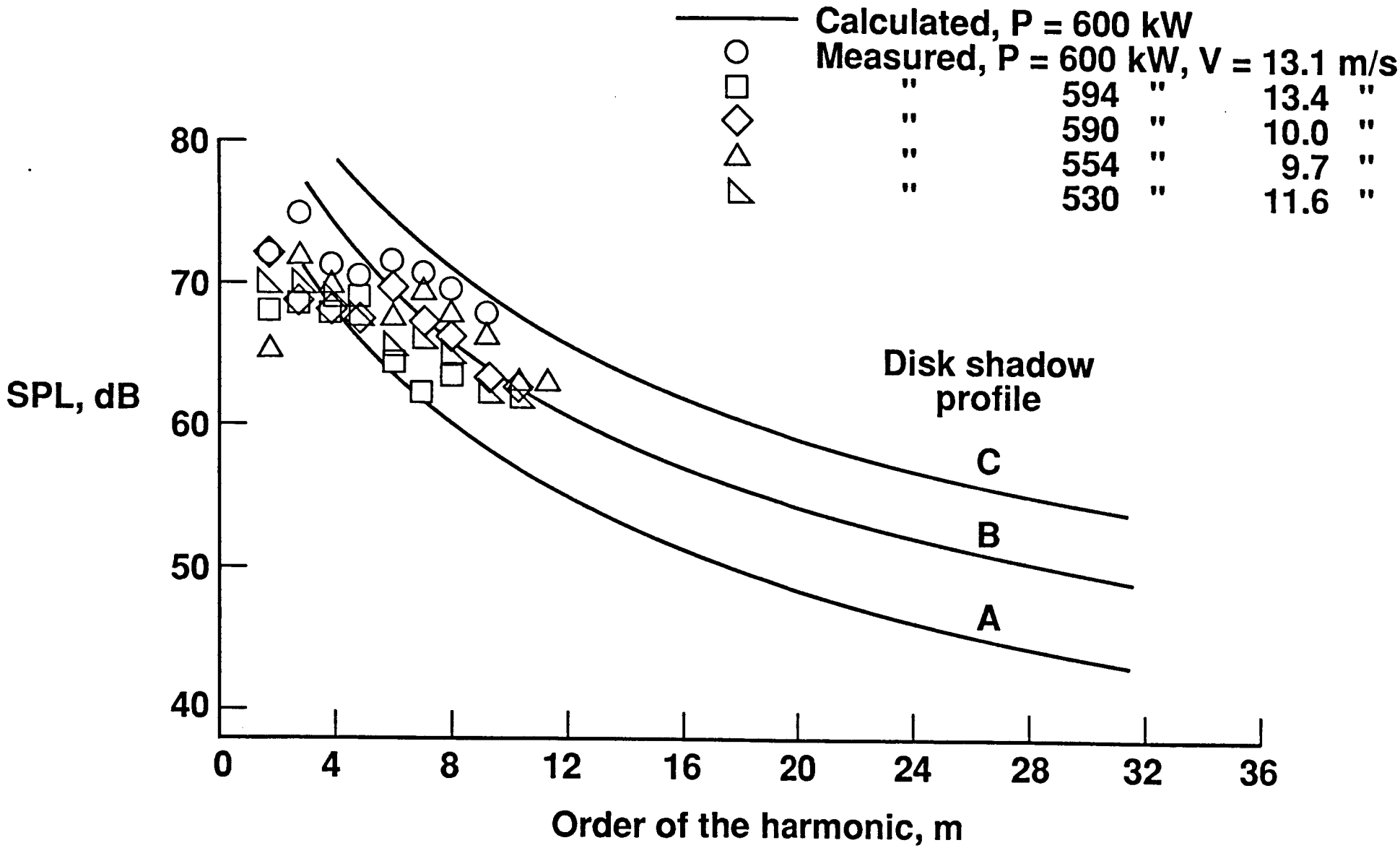

Figure 12. - Comparisons of measured rotational harmonic levels with calculated spectrum envelopes for assumed disk shadow profiles of figure 10. d = 65 m.

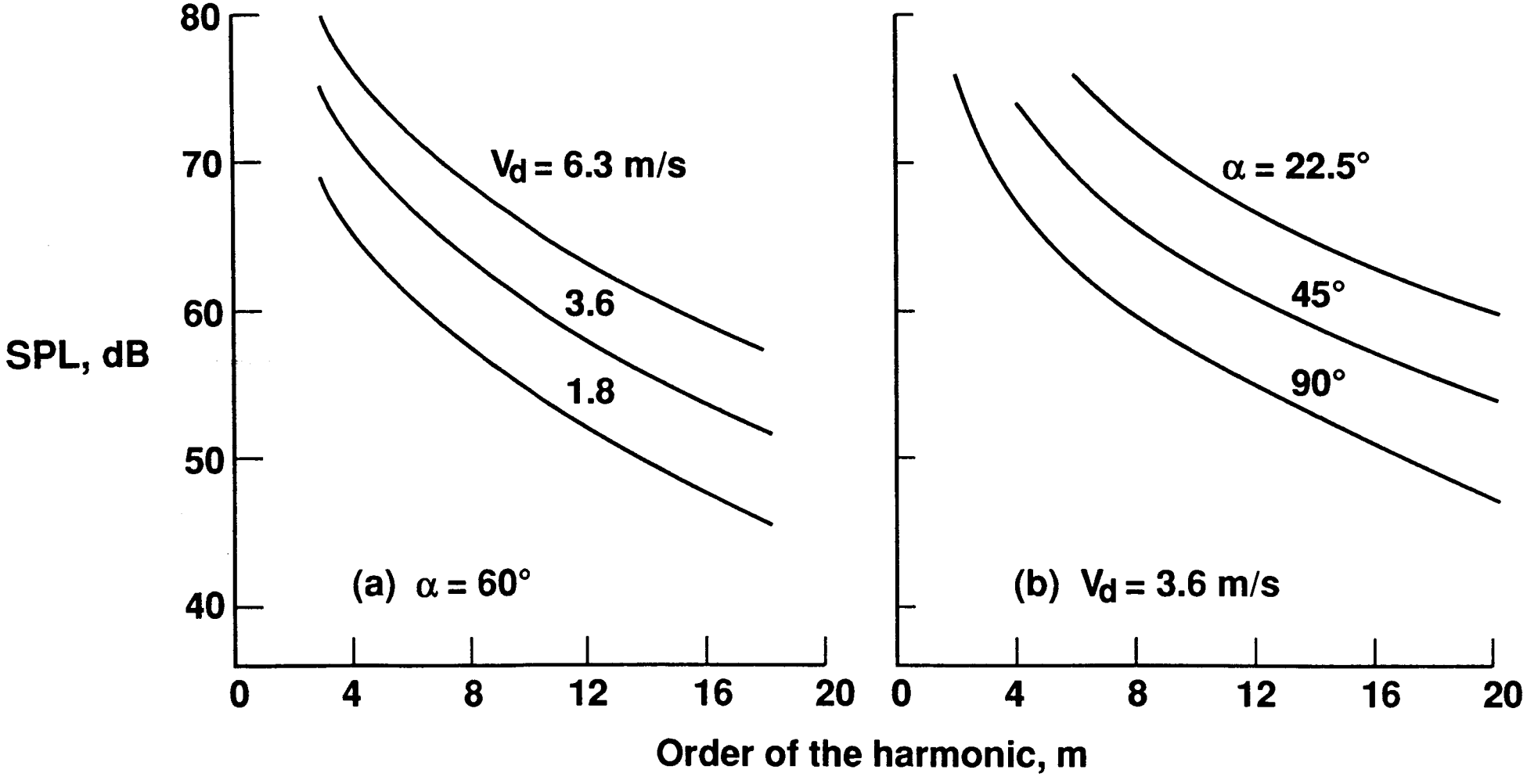

Figure 13. - Calculated effects of velocity deficit and disk shadow angle on the spectrum envelopes for the WWG-0600 machine. P = 600 kW, d = 65 m.

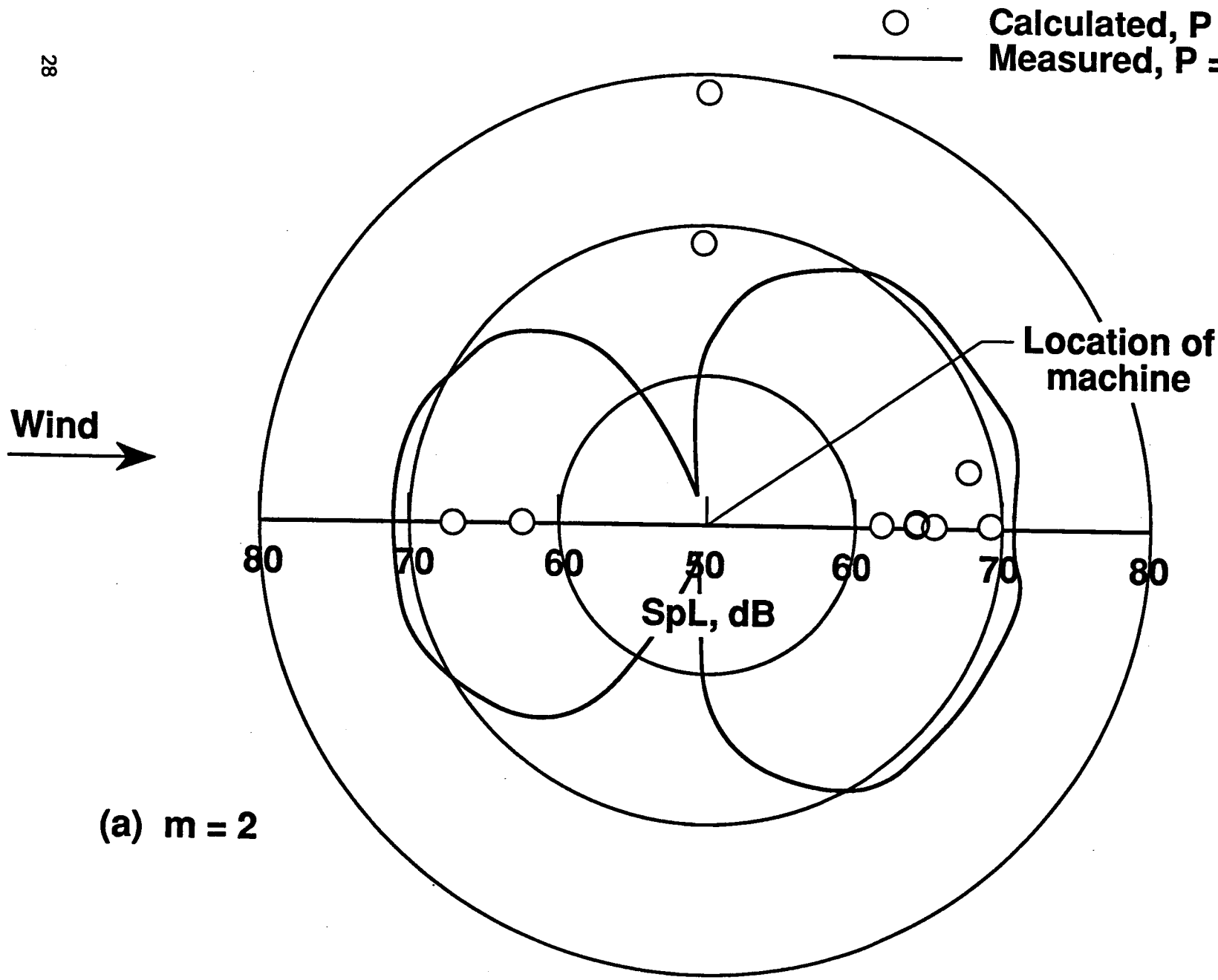

Figure 14. - Comparisons of measured and calculated sound pressure levels of three different rotational harmonics at various azimuth angles from the WWG-0600 machine, for assumed disk shadow profile B of figure 10. d=65 m.

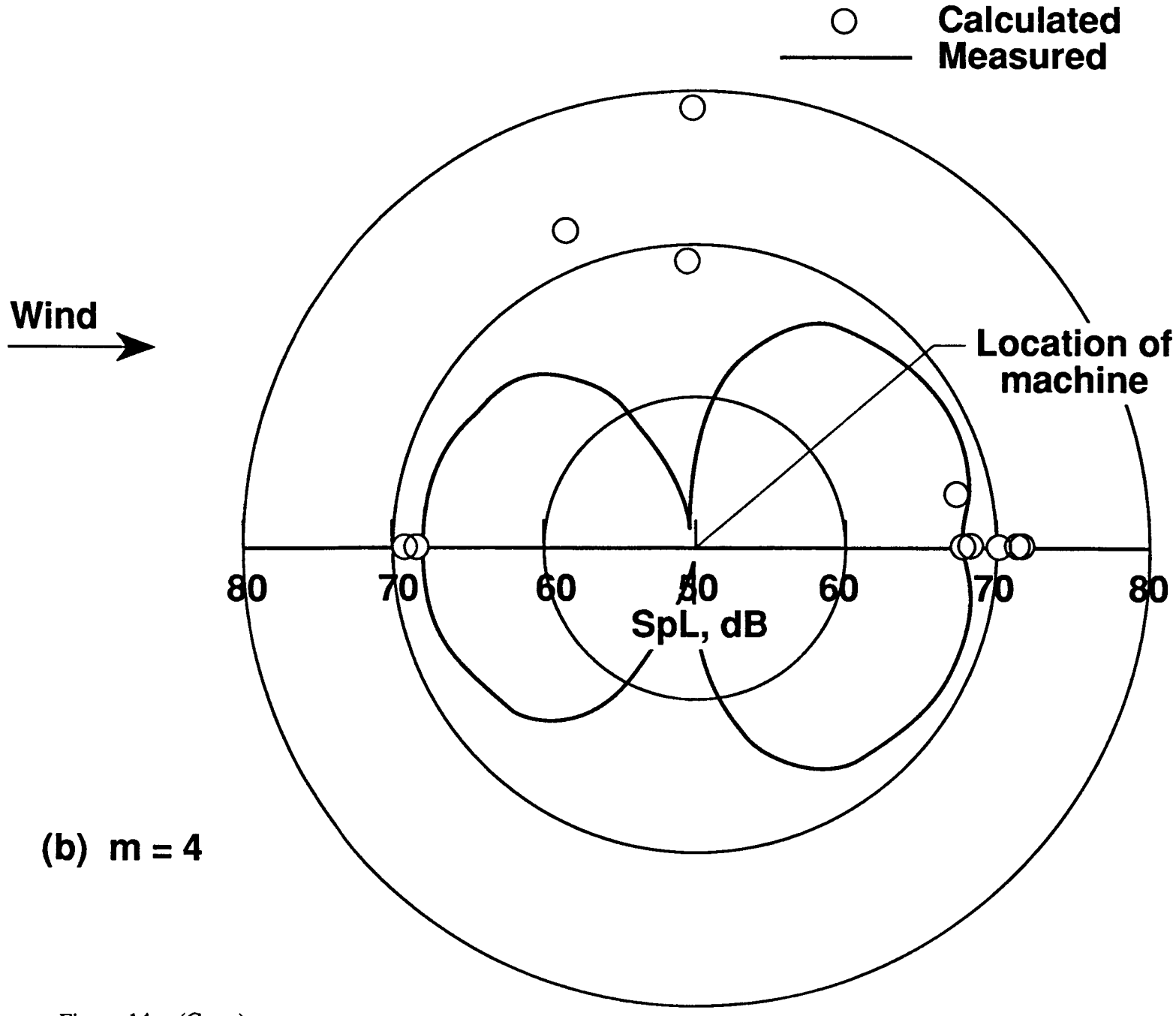

Figure 14. - (Cont.)

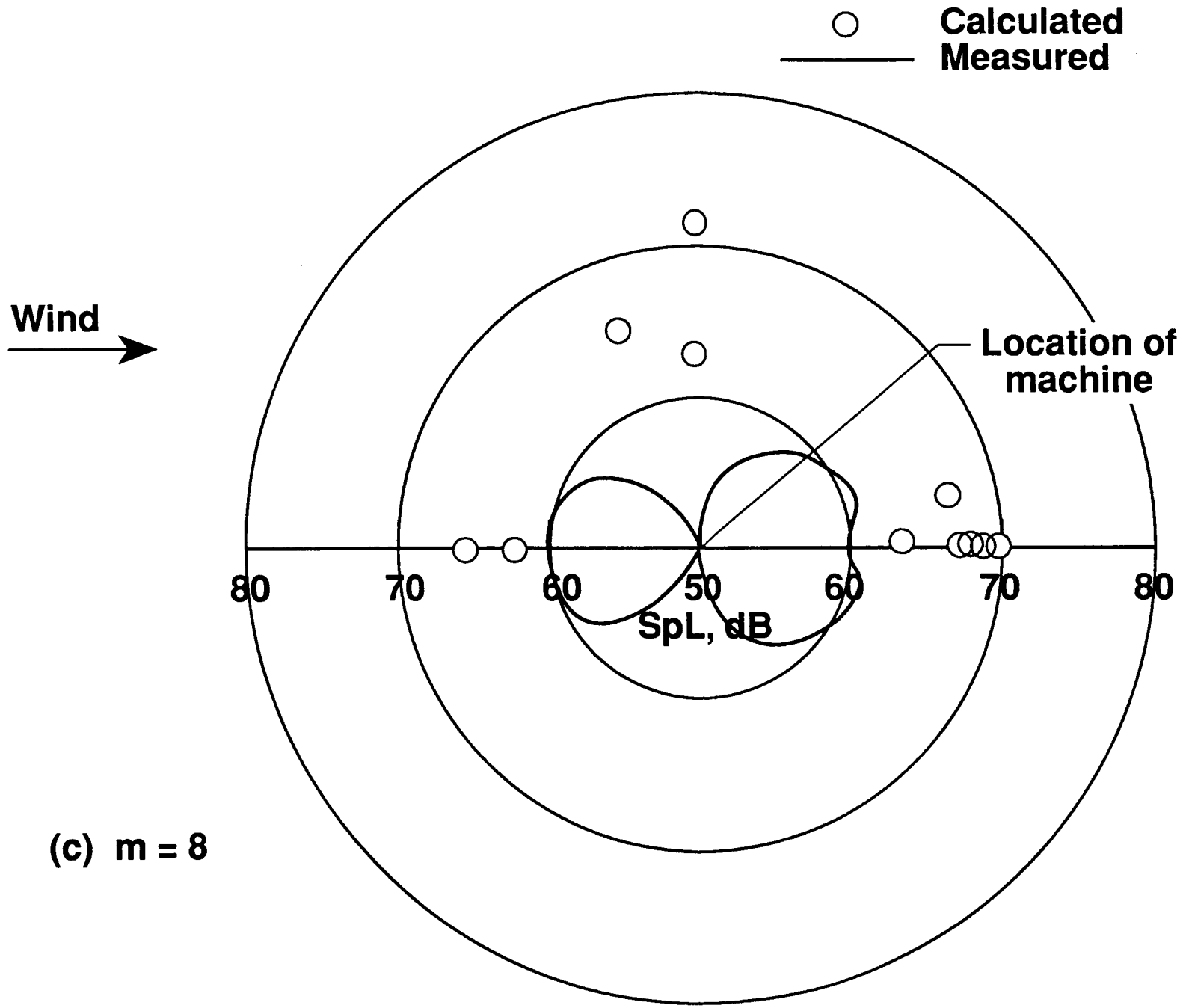

Figure 14. - (Concl.)

NASA
National Aeronautics and Space Administration

Report Documentation Page

1. Report No.	2. Government Accession No.	3. Recipient's Catalog No.
NASA TM-101576		

4. Title and Subtitle

Noise Radiation Characteristics of the Westinghouse WWG-0600 (600kW) Wind Turbine Generator

5. Report Date

July 1989

6. Performing Organization Code

7. Author(s)

Kevin P. Shepherd* and Harvey H. Hubbard**

8. Performing Organization Report No.

10. Work Unit No.

535-03-11-03

9. Performing Organization Name and Address

NASA Langley Research Center
Hampton, VA 23665-5225

11. Contract or Grant No.

13. Type of Report and Period Covered

Technical Memorandum

12. Sponsoring Agency Name and Address

National Aeronautics & Space Administration
Washington, DC 20546

14. Sponsoring Agency Code

15. Supplementary Notes

*Langley Research Center, Hampton, VA
**Planning Research Corporation, Hampton, VA

16. Abstract

Acoustic data are presented from five different WWG-0600 machines for the wind speed range 6.7-13.4 m/s, for a power output range of 51-600 kW and for upwind, downwind and crosswind locations. Both broadband and narrowband data are presented and are compared with calculations and with similar data from other machines.

Predicted broadband spectra are in good agreement with measurements at high power and underestimate them at low power. Discrete frequency rotational noise components are present in all measurements and are believed due to terrain induced wind gradients. Predictions are in general agreement with measurements upwind and downwind but underestimate them in the crosswind direction.

17. Key Words (Suggested by Author(s))	18. Distribution Statement
wind turbine acoustics noise generation noise prediction noise measurement	Unclassified - Unlimited Subject Category 71

19. Security Classif. (of this report)	20. Security Classif. (of this page)	21. No. of pages	22. Price
Unclassified	Unclassified	31	A03